

# Load on a wind turbine blade and its stress condition

Mária Čarnogurská<sup>1</sup>, Marián Lázár<sup>2</sup>, Romana Dobáková<sup>3</sup>, Jiří Marek<sup>4</sup>

<sup>1,2,3</sup>Department of Power Engineering, Faculty of Mechanical Engineering, Technical University of Košice, 042 00 Košice, Slovak Republic,

<sup>4</sup>VŠB – Technical University of Ostrava, Faculty of Metallurgy and Materials Engineering, Ostrava –Poruba, Czech Republic.

**Abstract** – The article provides an analysis of the stress and deformation conditions of NACA blade at wind speed of 3-12 m/s and in a parking position (over 20 m/s). The wind speed of 9 m/s and Poisson's glass-epoxy laminate with a value of 0.43 initiates yaw of the blade tip from the axis of rotation by 651 mm. Von Mises stress reaches a value of 75.58 MPa. Visualization of airflow around the blade demonstrates that flow separation occurs at the point of blade mounting in the hub and the speed is higher than airflow speed around the blade tip.

**Keywords** – the finite element method, visualization of air-flow, stress of the blade.

## I. INTRODUCTION

Wind power installations are used to convert kinetic energy of wind into electricity. This conversion can be performed in various ways, however, so-called Betz limit with a power coefficient of 0.593 cannot be surpassed. When the value of the coefficient is greater than 0.5, aerodynamic efficiency rises up to 85%. Precisely manufactured blades, e.g. NACA type blades, must be utilised in order to achieve such efficiency. This type of blades represents the most effective method how to generate the pressure difference required in a wind turbine rotor. Blades of this type can also reach a considerable proportion of the aerodynamic lift  $c_y$  to aerodynamic drag coefficient  $c_x$ . The values of both coefficients are affected by the angle of attack  $\alpha$ , which determines pressure distribution on the blade as well as its stress state.

## II. DETERMINATION OF AERODYNAMIC FORCE

Blade stress is a product of resultant aerodynamic force  $R$  (Fig. 1) and there are two methods of its calculation. Either by axial and tangential force or by means of drag and lift force. Axial force  $T$  can be determined by Equation (1) for a selected number of cross sections of the blade along its length (Fig. 2):

$$dT_i = (1/8) \cdot dc_{T_i} \cdot \rho \cdot \pi \cdot D^2 \cdot v_o^2 \quad (1)$$

where  $D$  – rotor diameter (m),  $v_o$ -wind speed,  $\rho$  - air density,  $c_T$  – axial force coefficient.

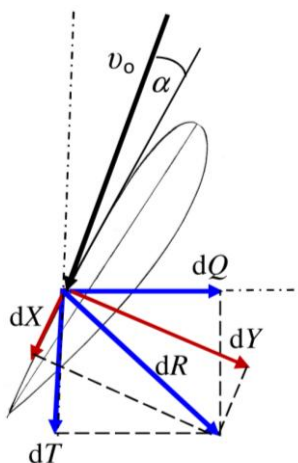


FIGURE 1: Forces on a blade element

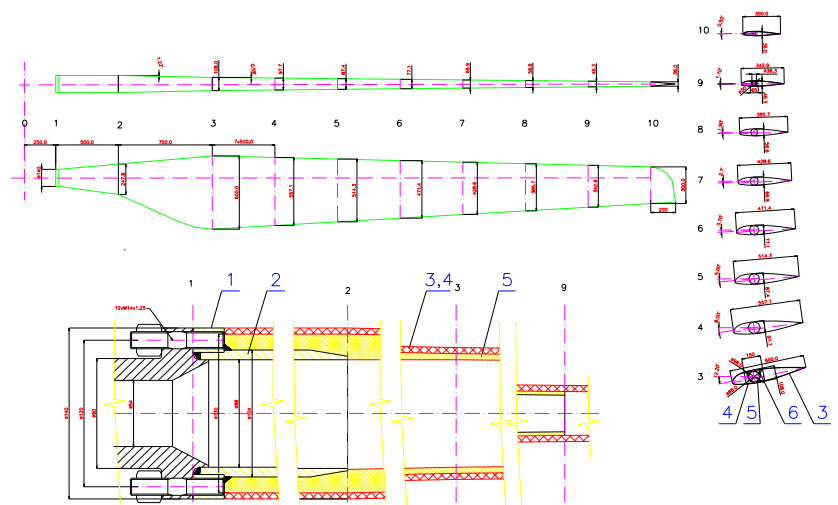


FIGURE 2: The geometry of a wind turbine rotor blade

Equation (2) can be used to determine elemental tangential force  $dQ$  for all investigated distances  $r_i$  from the axis of rotation employing known torque coefficient  $c_M$ :

$$dQ_i = \frac{dM_{ki}}{r_i} \quad (2)$$

$$\text{where } M_k = (1/16) \cdot c_M \cdot \rho \cdot \pi \cdot D^3 \cdot v_o^2 \quad (3)$$

Axial force coefficient  $c_T$  and torque coefficient  $c_M$  depend on the blade pitch angle and their courses are given in [2]. Elementary aerodynamic force  $dR_i$  can be then determined for the distances  $r_i$  from the axis of rotation as defined by equation (4):

$$dR_i = \sqrt{dT_i^2 + dQ_i^2} \quad (4)$$

The static effect of airflow on stress conditions was examined by the resultant aerodynamic force  $R$ , determined by integrating of elemental axial forces and tangential forces along the entire length of the blade. Calculation of aerodynamic forces by means of drag force and lift force is based on relationship (5) to (7). Drag force can be determined as follows:

$$X = \frac{1}{2} \cdot \rho \cdot c_x \cdot S_t \cdot v_o^2 \quad (5)$$

where  $S_t$  is an airfoil area - given as a product of the airfoil chord length and the height of a blade,  $\rho$  - air density,  $c_x$  - drag coefficient,  $v_o$  - air velocity. Lift force, which acts perpendicularly on the air speed, is a function of the lift coefficient  $c_y$ :

$$Y = \frac{1}{2} \cdot \rho \cdot c_y \cdot S_t \cdot v_o^2 \quad (6)$$

Relationship (6) indicates the resultant aerodynamic force  $R$  as follows:

$$R = \sqrt{X^2 + Y^2} \quad (7)$$

### III. RESULTS OF THE STUDY OF FORCE CONDITIONS ON THE BLADE

The rotor remains in the basic operational position at wind speeds from 3 to 9 m/s. Therefore, the load condition of the blade was analysed at maximum wind speed of 9 m/s. The calculation of stress condition was performed employing the FEM method (Finite Elements Method). Airflow around the blade is also visualised in this state.

The analysed blade has a length of 5000 mm. A geometric model of the blade for the structural analysis of a stress condition and deformation of the blade with the effect of wind of the speed of 9 m/s was developed by SOLID elements with a quadratic base function.

The calculation model of the blade contains 6610 elements in total. The boundary condition was defined by wind pressure acting onto the blade in a normal direction and the effect of centrifugal force and gravitational acceleration. Material properties were included separately for the metal cantilever beam and the coat of the blade as well as its internal epoxy-fiberglass reinforcement. The cantilever beam is made of material 12 021.1 (yield strength  $Re = 235$  MPa). When safety factor  $n=1.5$ , allowable stress for the beam is  $\sigma_{\text{dov}} = 157$  MPa. Epoxy-fiberglass has allowable stress  $\sigma_{\text{dov}} = 98$  MPa. Other material properties are shown in Table 1. Stress conditions were determined for the most unfavourable position of the blade in which gravitation and centrifugal force are of the same direction. Such case occurs when a blade tip points towards the ground.

**TABLE 1**  
**MATERIAL PROPERTIES**

	steel 12 021.1	epoxy-fiberglass
modulus of elasticity $E$ (MPa)	$2,6 \cdot 10^5$	$0,048 \cdot 10^5$
Poisson number $\mu$ (-)	0.28	0.28% to 0.43%
density $\rho$ (kg/m <sup>3</sup> )	7850	1950

Fig. 3 shows deformation of the blade along its length in steady state. Maximum yaw of the blade tip from the axis of rotation is  $\delta = 651$  mm. The blade is attached to a root attachment made of steel. Fig. 4 shows the strain in the root region of

the blade. The maximum value of reduced Von Mises strain at the end of the root section is approximately 60 MPa (yellow). Deformation of the blade increases stress within its material, which is epoxy-fiberglass.

The global assessment of a stress condition of the blade as a whole (comprising of a steel attachment and reinforcements) yields a stress state of reduced Misses strains with a value of 75.58 MPa. Such state corresponds with the solution using Poisson number with a value  $\mu = 0.43$ . Tab. 2 shows the values of stress on the blade under static load for four selected wind speeds and two Poisson numbers.

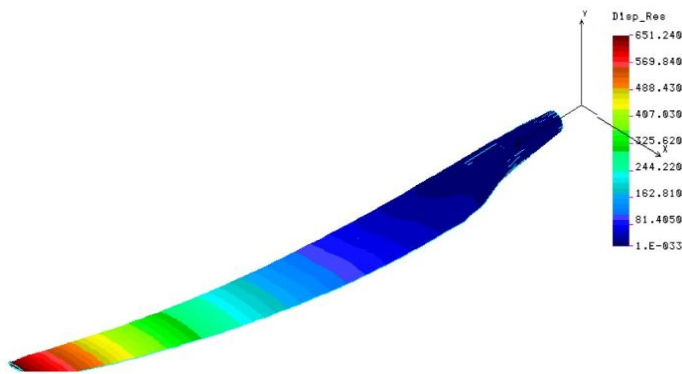


**FIGURE 3: Stress state and blade deformation at wind speed  $v_0 = 9$  m/s**

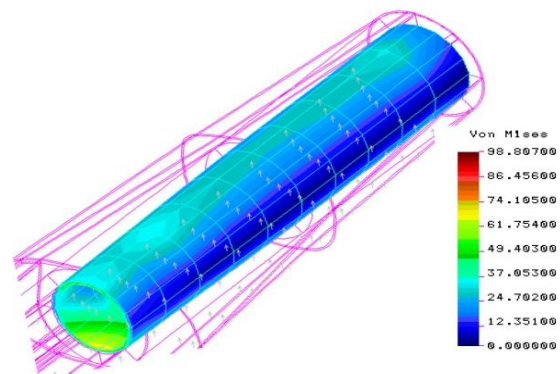


**FIGURE 4: Stress in the root section**

The wind turbine should work in the environment where wind speeds range between 3 and 9 m/s. Considered tip-speed ratio is  $\lambda = 5.75$ . Axial force coefficient  $c_T$  on the blade profile is about 0.5. If a wind speed exceeds 20m/s, the control system adjusts the pitch angle  $\phi$ , so at wind speed of 12m/s revolution speed remain 2 rev/s and the power output is about 15 kW. This power output is maintained constant until wind speed exceeds 20m/s (blade pitch angle is adjusted depending on the wind speed to keep the power output constant at all times). When wind speed is over 20 m/s, the blade pitch angle at the tip  $\phi$  is set to  $60^\circ$  and the propeller will stall. This way the energy of wind passes through the rotor without being exploited and stress in the turbine is equivalent to the stress in an operational position at wind speed of 3m/s (Tab. 2).

**TABLE 2  
STRESS AND DEFORMATION OF THE ROTOR BLADE WHEN CONSIDERING STATIC LOAD**

$v_0$ (m/s)	<i>Poisson number</i>			
	0.43		0.28	
	$\sigma$ (MPa)	$\delta$ (mm)	$\sigma$ (MPa)	$\delta$ (mm)
3	12.91	118.87	11.705	119.15
9	<b>75.578</b>	<b>651.24</b>	<b>68.77</b>	<b>653.49</b>
12	124.1	1070.4	112.46	1073.3
20	12.55	95.5	11.72	95.8

Airflow around the blade was modelled by software called FLUENT. The chord divides the airfoil surface into a downwind and upwind side. The downwind side has a smaller surface area ( $S_n = 2.1393 \text{ m}^2$ ) than the upwind side ( $S_n = 2.1989 \text{ m}^2$ ). Airflow around the blade causes negative pressure on the upwind side proportional to the wind speed. As the wind speed increases, air streamlines separate from the airfoil (wake occurs) and negative pressure is produced in the area of separation. There is always overpressure on the downwind side. Its amount mainly depends on the blade pitch angle relative to the plane of rotation, but also on airflow speed. It is possible to determine the amount of force exerted on the downwind ( $F_n$ ) and upwind ( $F_z$ ) side for a given winds speed and pitch angle. A particular value of force on a given area depends on the amount of static ( $p_s$ ) and dynamic ( $p_d$ ) pressure. Surface integration of the individual pressures or the total pressure ( $p_{tot} = p_s + p_d$ ) can be used to determine the forces on both surfaces. Their difference yields resultant aerodynamic force  $R$  according to equation (8):

$$R_{tot} = \int_S dR_{tot} = \int_S p_{tot} dS = \int_S (p_s + p_d) dS \tag{8}$$

or

$$R_{tot} = \sum_{i=1}^n p_{i,tot} \cdot S_i \tag{9}$$

Based on the resultant aerodynamic force, resistance coefficient  $c$  can be determined based on formula (10).

$$c = \frac{2 \cdot R_{tot}}{\rho \cdot S_t \cdot v_0^2} \tag{10}$$

where  $S_t$  blade surface area obtained as the product of the chord and the height of the blade.

Table 3 presents the values of the resultant forces, the static pressure  $R_s$ , dynamic pressure  $R_d$  total pressure  $R_{tot}$  acting on the downwind and upwind side of the blade.

**TABLE 3**  
**Pressures and forces on the downwind and upwind side of the blade at a wind speed  $v_0 = 9$  m/s and blade pitch angle  $12^\circ$**

	$R_s$ (N)	$R_d$ (N)	$R_{tot}$ (N)	$p_s$ (Pa)	$p_d$ (Pa)	$p_{tot}$ (Pa)
$S_z$ (m <sup>2</sup> )	-606.734	121.467	-469.647	-275.929	55.241	-213.585
$S_u$ (m <sup>2</sup> )	397.369	250.348	641.886	185.746	117.022	300.043
$\sum S$ (m <sup>2</sup> )	1004.103	371.815	1111.5333	461.675	172.263	513.627

#### IV. CONCLUSION

The examined stress and load conditions are on the turbine blade of a wind power plant to be located in the area with lower wind-energy potential. The maximum assumed wind speeds 30m above ground range between 5 - 9 m/s.

The airflow around the root attachment is shown in Fig. 5 and the blade tip in Fig. 6. A wake occurs on the upwind side of the root section and the flow separates from the surface of the root attachment. This is due to the fact that the root attachment has a cylindrical shape, which is, in terms of airflow, the least favourable shape. The wind speed on the upwind side reaches up to 37.6 m/s. The wake is weaker on the blade tip due to a more suitable airfoil profile. The maximum speed is about 24 m/s.

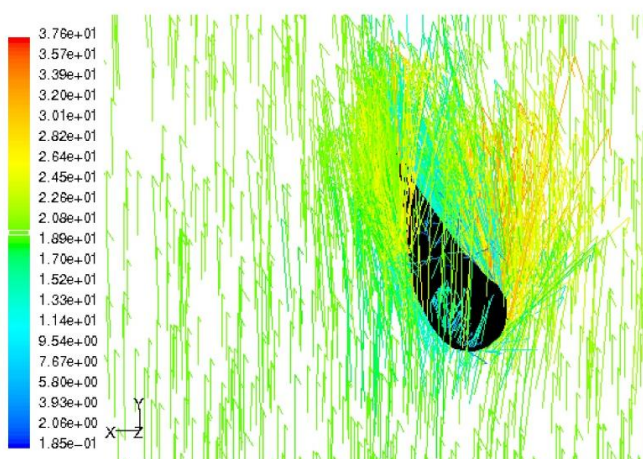


**FIGURE 5 AIRFLOW AROUND THE BLADE ATTACHMENT**

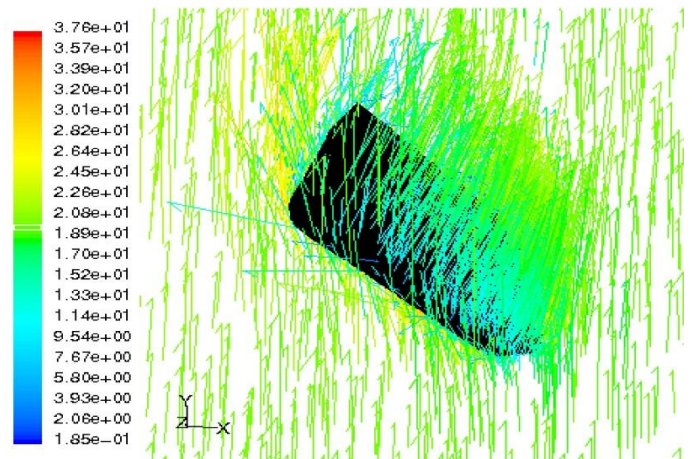


**FIGURE 6 AIRFLOW AROUND THE BLADE TIP**

#### ACKNOWLEDGEMENTS

The paper has been produced as a part of a project KEGA No. 003TUKÉ-4/2016

**REFERENCES**

- [1] D. Rozehnal, 2000, Aerodynamic loading of wind motor with a horizontal rotation axis, *Wind Power*, 2 (2000) pp. 13-15.
- [2] M. Čarnogurská, D. Rozehnal , Aerodynamic characteristics of wind power plant's rotor with a blade profile of type NACA, Proc. from the 2<sup>nd</sup> conference Small water systems and alternative sources of power, DT Košice, 2003, pp. 199-204.
- [3] Le Gouriér's, D.: *Wind power plants, theory and design*. Pergamon Press, Toronto-Sydney-Frankfurt. 1982.
- [4] M. Čarnogurská, M., Kozubková, M. Bojko, Flow over wind-mill rotor blade in a parking position and its stress state. *ACTA MECHANICA SLOVACA*, 3 (2003) pp. 323 -330.
- [5] COSMOS/M, User's Guide, Release 2.6.